Mycosphere 9(5): 999–1013 (2018) www.mycosphere.org ISSN 2077 7019
Article
Doi 10.5943/mycosphere/9/5/4

Additions to *Pestalotiopsis* in Taiwan

Ariyawansa HA[1] and Hyde KD[2]

[1]*Department of Plant Pathology and Microbiology, College of Bio-Resources and Agriculture, National Taiwan University, Taiwan*
[2]*Center of Excellence in Fungal Research, Mae Fah Luang University, Chiang Rai 57100, Thailand*

Ariyawansa HA, Hyde KD 2018 – Additions to *Pestalotiopsis* in Taiwan. Mycosphere 9(5), 999–1013, Doi 10.5943/mycosphere/9/5/4

Abstract

As part of fungal exploration of Taiwan, we found several pestalotioid taxa from Taipei Botanical Gardens, Zhongzheng District. Based on single- and multi-locus phylogenies using internal transcribed spacer, β–tubulin and partial translation elongation factor 1–α gene regions, along with morphological features, these species fit into two novel taxa of *Pestalotiopsis sensu stricto* and are proposed herein as *Pestalotiopsis formosana* and *P. neolitseae*. *Pestalotiopsis formosana* and *P. neolitseae* were isolated from dead grass and living leaves of *Neolitsea villosa* respectively. These two novel species are morphologically comparable with *Pestalotiopsis sensu stricto* in having concolourous median cells, but differ from the phylogenetically related species in the size of the conidia, the number of apical appendages, the length of basal appendages, plus ecology and distribution. The results of pathogenicity testing revealed that *Pestalotiopsis neolitseae* is capable of causing leaf spots on *Neolitsea villosa* and to the best of our knowledge, this is the first record of *Pestalotiopsis* species associated with leaf spots of *Neolitsea villosa* in Taiwan.

Key words – 2 new taxa – New record – New species – Pestalotioid species – Phylogeny – phytopathogenic fungi

Introduction

The genus *Pestalotiopsis* was introduced by Steyaert (1949) to accommodate pestalotioid taxa with 5-celled conidia and is presently placed in Sporocadaceae of Amphisphaeriales (Wijayawardene et al. 2017, 2018). With the advent of molecular data, extensive improvements have been incorporated over the past decade in unravelling the phylogenetic resolution within *Pestalotiopsis* and its allied genera (Maharachchikumbura et al. 2014). Maharachchikumbura et al. (2014) introduced two new genera namely *Neopestalotiopsis* and *Pseudopestalotiopsis* to accommodate pestalotiopsis-like species based on morphology, coupled with molecular data. Furthermore, Maharachchikumbura et al. (2014) concluded that these three genera can be identified based on the conidiogenous cells and colour of their median conidial cells, thus the pestalotiopsis-like taxa having concolourous median cells were retained in *Pestalotiopsis sensu stricto* (Maharachchikumbura et al. 2014). Taxa having dark coloured concolourous median cells were categorised in *Pseudopestalotiopsis* while pestalotioid taxa with versicolourous median cells were placed under *Neopestalotiopsis* (Maharachchikumbura et al. 2014). Currently, the genus

Submitted 16 August 2018, Accepted 7 September 2018, Published 10 October 2018 2018
Corresponding Author: Hiran A. Ariyawansa – e-mail – ariyawansa44@ntu.edu.tw

Pestalotiopsis comprises 52 phylogenetically verified species, which have been reported from various hosts and habitats (Liu et al. 2017, Maharachchikumbura et al. 2014).

We have been studying pestalotioid taxa from various hosts and habitats in Taiwan to provide the stable molecular based systematic to this chemically diverse fungal group (Ariyawansa et al. 2018, Tsai et al. 2018). During our ongoing investigation, several fungal isolates, which are morphologically comparable to *Pestalotiopsis sensu stricto* (Maharachchikumbura et al. 2014) were collected from Taipei Botanical Gardens, Zhongzheng District in Taiwan. The aim of this paper is to investigate the taxonomic position of the isolated pestalotioid taxa based on morphology and molecular phylogenetic analyses of internal transcribed spacer (ITS), β-tubulin (*tub2*) and partial translation elongation factor 1-α gene (*tef1*).

Materials & Methods

Sample collection and fungal isolation

Thirty naturally infected *Neolitsea villosa* (Blume) Merr. leaves and 30 dead grass samples were collected from the Taipei Botanical Gardens, Zhongzheng District, Taipei City, Taiwan, during 2017–2018. The samples were brought to the laboratory in Ziplock plastic bags. The specimens were processed and examined following the method described in Ariyawansa et al. (2014, 2016a, b). Fresh materials were observed under a Motic SMZ 168 dissecting microscope to locate and isolate fruiting bodies. Hand sections of the fruiting structures were mounted in water for microscopic studies and photomicrography. Isolations were made from single conidia, following an altered method of Ariyawansa et al. (2018). Morphological descriptions were prepared for isolates cultured on 2% potato dextrose agar (PDA; Difco). Conidiomatal growth was observed on WA with double-autoclaved pine needles located onto the agar surface (PNA). Cultures were incubated at room temperature (25 °C) for 7 days. Microscopic slide preparations were carried out in distilled water, and as a minimum 30 measurements per structure were noted and observed with an Olympus BX51 microscope using differential interference contrast (DIC) illumination. Taxonomic descriptions are deposited in Facesoffungi (Jayasiri et al. 2015) and nomenclature details in MycoBank. New taxa are decided based on recommendations defined by Jeewon & Hyde (2016).

Voucher specimens are deposited in the herbarium of Department of Plant Pathology and Microbiology, National Taiwan University (NTUH). Living cultures are deposited at the Department of Plant Pathology and Microbiology, National Taiwan University Culture Collection (NTUCC).

DNA extraction, PCR amplification and sequencing

Single conidial isolates were grown on PDA for 28 days at 25 °C in the dark. Genomic DNA was extracted from the growing mycelium following the method described in Ariyawansa et al. (2018). The PCR amplification process was carried out as described by Tsai et al. (2018). Primer sets used for these genes were as follows: ITS5/ITS4 (White et al. 1990), BT2A/BT2B (Glass & Donaldson 1995, O'Donnell & Cigelnik 1997), and EF1-728F/EF2 (Rehner 2001, Liu et al. 2017) respectively. The PCR reactions for amplification of ITS (Schoch et al. 2012), were accomplished under regular conditions (White et al. 1990, Stielow et al. 2010). Amplification of *tub2* and *tef1* followed the protocol of Maharachchikumbura et al. (2014). The PCR products were visualized on 1.5% agarose electrophoresis gels stained with SYBR safe DNA gel stain. Purification and sequencing of PCR products was carried at Genomics, New Taipei, Taiwan. Consensus sequences from sequences generated from forward and reverse primers were obtained via DNASTAR Lasergene SeqMan Pro v.8.1.3. Sequences are placed at NCBI GenBank under the accession numbers provided in Supplementary Table 1.

Sequence alignment and phylogenetic analysis

Multiple sequence alignments were produced with MAFFT v. 6.864b (http://mafft.cbrc.jp/alignment/server/index.html). The alignments were tested visually and

improved manually where needed. Regions covering many leading or trailing gaps were discarded from the alignments prior to tree building. All sequences obtained from GenBank and used by Chen et al. (2018), Liu et al. (2017), Maharachchikumbura et al. (2014), Nozawa et al. (2017) are listed in Supplementary Table 1. To decide closely allied taxa, single gene phylogenies were inferred for ITS, *tub2* and *tef1* and lastly subjected to a multigene combined analysis.

MrModeltest v. 2.3 (Nylander 2004) under the Akaike Information Criterion (AIC) was implemented in PAUP v. 4.0b10 used to determined evolutionary models for phylogenetic analyses. Comparison of the alignment properties and nucleotide substitution models for each gene locus are provided in Table 1.

A maximum likelihood analysis was done at the CIPRES webportal (Miller et al. 2010) using RAxML–HPC2 on XSEDE (v 8.2.8) with default parameters and bootstrapping with 1000 replicates (Stamatakis 2014). The resulting replicates were marked on to the best scoring tree acquired previously. Maximum Likelihood bootstrap values (ML) equal or greater than 70 % are given below or above each node (Fig. 1).

Markov Chain Monte Carlo sampling (MCMC) implemented in MrBayes v. 3.0b4 (Huelsenbeck & Ronquist 2001) was used to calculate Posterior probabilities (BP) (Rannala & Yang 1996, Zhaxybayeva & Gogarten 2002). Six simultaneous Markov chains were initially run for 1×10^{10} generations and every 100^{th} generation a tree was sampled (critical value for the topological convergence diagnostic set to 0.01, options of "stoprule = yes" and "stopval = 0.01"). MCMC heated chain was set with a "temperature" value of 0.15. The distribution of log-likelihood scores was observed to decide stationary phase for each search and to check if further runs were required to reach convergence, using the program Tracer 1.5 (Rambaut & Drummond 2007). All sampled topologies below the asymptote (20%) were removed as part of a burn-in process, the remaining trees were used for computing posterior probabilities in the majority rule consensus tree. BP equal or greater than 0.95 are given below or above each node (Fig. 1).

In order to decide the species boundaries in *Pestalotiopsis sensu stricto*, we applied the principles of Genealogical Concordance Phylogenetic Species Recognition (GCPSR) (Taylor et al. 2000, Dettman et al. 2003). Dettman et al. (2003) underlined that species should be acknowledged if they satisfy one of two criteria: genealogical concordance or genealogical non-discordance. Clades were genealogically concordant if they were existing in at least some of the gene trees and genealogically non–discordant if they were strongly supported (ML≥70%; BP≥0.95) in a single loci and not contradicted at or above this level of support in any other single gene tree. This standard prohibited poorly supported non–monophyly at one locus from undermining well–supported monophyly at another locus. Phylogenetic trees and data files were viewed in MEGA v. 5 (Tamura et al. 2011), TreeView v. 1.6.6 (Page 2001) and FigTree v. 1.4 (Rambaut & Drummond 2008).

Pathogenicity test

The pathogenicity of NTUCC 17–011 and NTUCC 17–012 isolates were tested on healthy leaves of *Neolitsea villosa* obtained from the initial collection sites at Taipei Botanical Garden, Taipei city, Taiwan. The upper and lower sides of leaves were sterilized with 70% ethanol. For each isolate, 15 leaves on *Neolitsea villosa* leaves were artificially inoculated. An agar plug (1 cm diam) with mycelium was cut from the border of five days-old culture grown on PDA medium (25 °C). The leaves were separated into three groups, each with five leaves. The first collection of leaves was wounded by pin-pricking and inoculated by agar plugs (1 cm diam) with fungal mycelium. Agar plugs with fungal mycelium were located on the surface of a second group comprising unwounded leaves. The leaves of control was not pin-pricked and was inoculated with PDA agar plugs without fungal mycelium. The inoculated test leaves were kept in sterile, moist plastic boxes for 14 days. Observations on the growth of disease symptoms were noted on a daily basis. In order to prove pathogenicity, the inoculated fungi were re-isolated from leaves showing lesions, and the identity of the re-isolated fungi was confirmed by sequencing the ITS, *tub2* and *tef1* loci as described above.

Results

Phylogeny

The topologies of the developed trees for each gene locus were compared manually, to ensure that the general tree topology of the single gene alignments, were comparable to each other and to that of the tree received from the concatenated alignment. The ML analyses showed similar tree topologies and were similar to those obtained in the Bayesian analyses. The results of the molecular phylogenetic analyses are supplied below (Fig. 1).

After exclusion of poorly aligned sites from each locus, the final concatenated data matrix comprised 1888 characters (ITS 559, *tub2* 781 and *tef1* 548) from 97 taxa.

The Bayesian analysis resulted in 50000 trees after 50000000 generations after the topological convergence. The first 10000 trees, representing the burn–in phase of the analyses were discarded, while the remaining trees were used for calculating posterior probabilities in the majority rule consensus tree.

A best scoring RAxML tree resulted with the value of Likelihood: –11258.033741. Phylogenetic trees obtained from ML and Bayesian analysis yielded trees with similar overall topology at the species level in arrangement with earlier studies based on ML and Bayesian analysis (Chen et al. 2018, Maharachchikumbura et al. 2014).

In both ML and Bayesian analyses, clade containing the two strains of *Pestalotiopsis* NTUCC 17–009 and NTUCC 17–010 form a distinct clade with high statistical support and neighbouring to clade representing *Pestalotiopsis parva* (CBS 278.35 and CBS 265.37) in both single locus and concatenated datasets analysis. Therefore, the new lineage is introduced here as the new species *Pestalotiopsis formosana*. Besides, in both single– and multi–gene phylogeny, the two strains of *Pestalotiopsis* NTUCC 17–011 and NTUCC 17–012 form a separate lineage with high statistical support and basal to *Pestalotiopsis jinchanghensis* (LC6636 and LC8190) clade in both ML and Bayesian analyses. Hence, the novel taxon *Pestalotiopsis neolitseae* is proposed to place taxa in the genus *Pestalotiopsis.*

Table 1 Evaluation of alignment properties of genes and nucleotide substitution models used in the phylogenetic analysis.

Genes /loci	*tef*	ITS	*tub*
Alignment strategy (MAFFT v6)	FFT-NS-I+manual	FFT-NS-I+manual	FFT-NS-I+manual
Nucleotide substitution models for Bayesian analysis (determined by MrModeltest)	GTR+G	GTR+G	GTR+G

Taxonomy

Pestalotiopsis formosana Ariyawansa & K.D. Hyde, sp. nov.

MycoBank number: MB827597; Facesoffungi number: FoF04937

Etymology – *formosana* an alternative name used for Taiwan, where this taxon was collected.

Saprobic on grass. Sexual morph: undetermined. Asexual morph: *Conidiomata* on PDA pycnidial, globose or lenticular, solitary or aggregate, immersed or semi–immersed, exuding black slimy conidial mass on the surface of mycelia. *Conidiophores* reduce to conidiogenous cells, when present, branched or unbranched, septate, hyaline. *Conidiogenous cell* discrete, cylindrical to subcylindrical, lageniform, hyaline, tapering to a thin neck, smooth, (5–)9–15(–19) × (2–)2–3(–4) μm, $\bar{x}$ ± SD = 11 ± 3.5 × 2 ± 0.4 μm, proliferating 1–4 times percurrently, collarette present. *Conidia* fusoid, straight to slightly curved, 4–septate, (15–)18–22(–26) × (5–)6–7 μm, $\bar{x}$ ± SD = 20 ± 2.1 × 6 ± 0.5 μm; basal cell obconic, cylindrical, with or without a truncate base, hyaline,

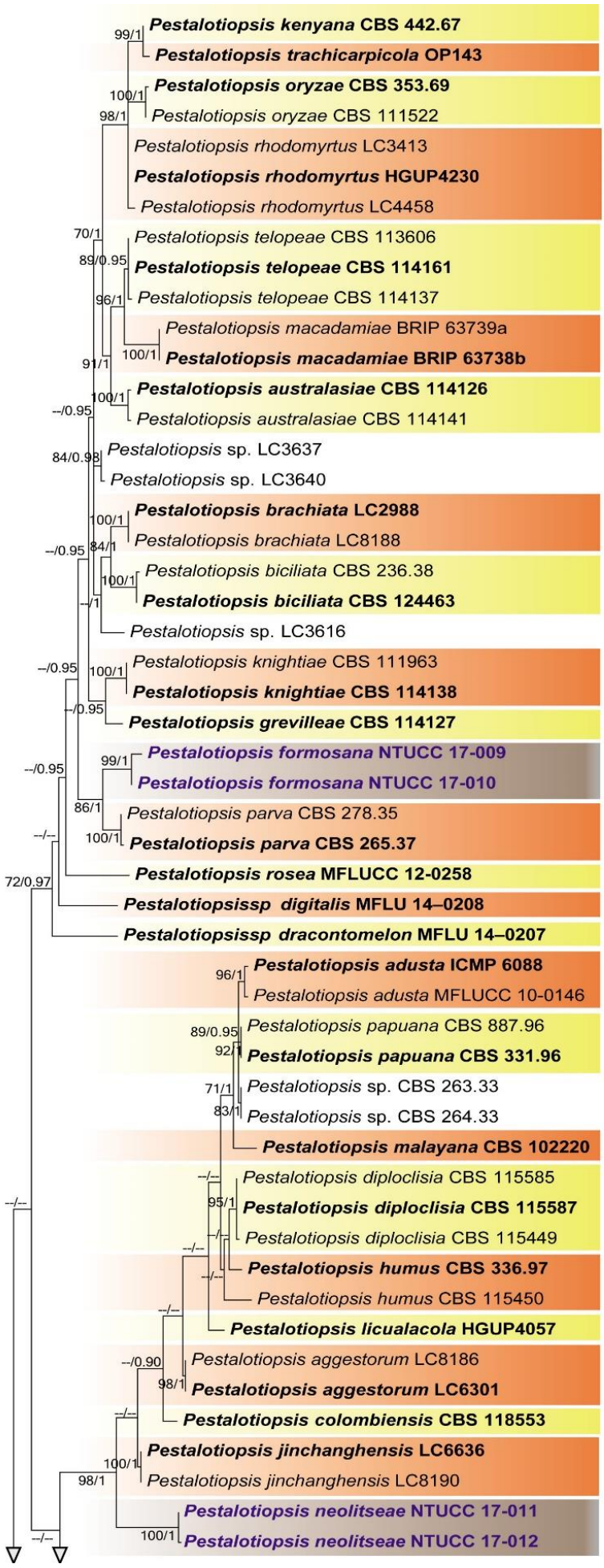
Pestalotiopsis kenyana CBS 442.67
Pestalotiopsis trachicarpicola OP143
Pestalotiopsis oryzae CBS 353.69
Pestalotiopsis oryzae CBS 111522
Pestalotiopsis rhodomyrtus LC3413
Pestalotiopsis rhodomyrtus HGUP4230
Pestalotiopsis rhodomyrtus LC4458
Pestalotiopsis telopeae CBS 113606
Pestalotiopsis telopeae CBS 114161
Pestalotiopsis telopeae CBS 114137
Pestalotiopsis macadamiae BRIP 63739a
Pestalotiopsis macadamiae BRIP 63738b
Pestalotiopsis australasiae CBS 114126
Pestalotiopsis australasiae CBS 114141
Pestalotiopsis sp. LC3637
Pestalotiopsis sp. LC3640
Pestalotiopsis brachiata LC2988
Pestalotiopsis brachiata LC8188
Pestalotiopsis biciliata CBS 236.38
Pestalotiopsis biciliata CBS 124463
Pestalotiopsis sp. LC3616
Pestalotiopsis knightiae CBS 111963
Pestalotiopsis knightiae CBS 114138
Pestalotiopsis grevilleae CBS 114127
Pestalotiopsis formosana NTUCC 17-009
Pestalotiopsis formosana NTUCC 17-010
Pestalotiopsis parva CBS 278.35
Pestalotiopsis parva CBS 265.37
Pestalotiopsis rosea MFLUCC 12-0258
Pestalotiopsissp digitalis MFLU 14–0208
Pestalotiopsissp dracontomelon MFLU 14–0207
Pestalotiopsis adusta ICMP 6088
Pestalotiopsis adusta MFLUCC 10-0146
Pestalotiopsis papuana CBS 887.96
Pestalotiopsis papuana CBS 331.96
Pestalotiopsis sp. CBS 263.33
Pestalotiopsis sp. CBS 264.33
Pestalotiopsis malayana CBS 102220
Pestalotiopsis diploclisia CBS 115585
Pestalotiopsis diploclisia CBS 115587
Pestalotiopsis diploclisia CBS 115449
Pestalotiopsis humus CBS 336.97
Pestalotiopsis humus CBS 115450
Pestalotiopsis licualacola HGUP4057
Pestalotiopsis aggestorum LC8186
Pestalotiopsis aggestorum LC6301
Pestalotiopsis colombiensis CBS 118553
Pestalotiopsis jinchanghensis LC6636
Pestalotiopsis jinchanghensis LC8190
Pestalotiopsis neolitseae NTUCC 17-011
Pestalotiopsis neolitseae NTUCC 17-012

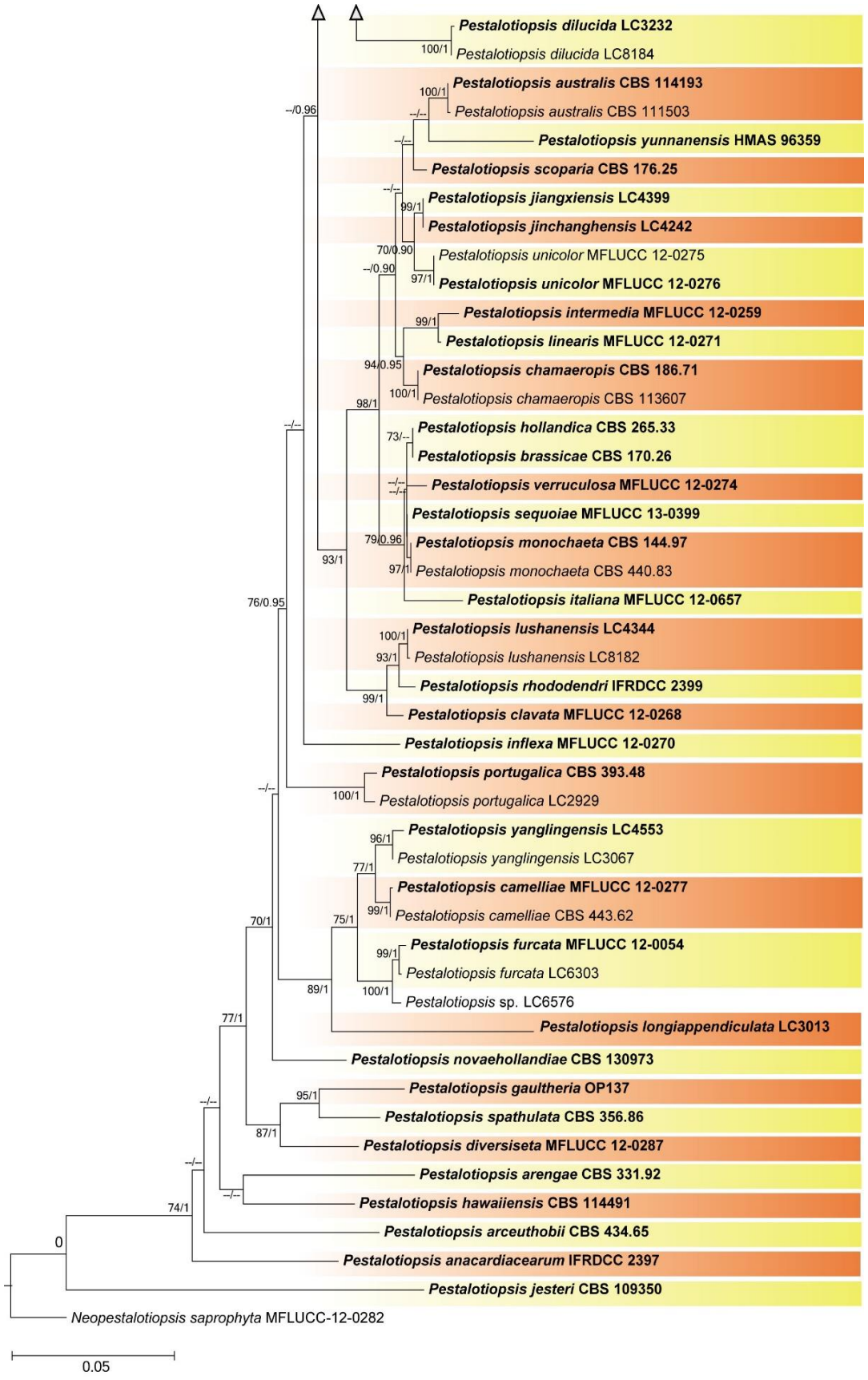

Figure 1 – RAxML tree obtained from the concatenated DNA sequence data of ITS, *tub* and *tef1* genes. The novel isolates are shown in blue. Bayesian posterior probabilities (PP) ≥ 0.95 and ML bootstrap values (BS) ≥70 % are given at the nodes. The scale bar shows the number of estimated substitutions per site. *Neopestalotiopsis saprophyta* (MFLUCC–12–0282) was used as outgroup for rooting the tree. Taxa representing ex–type cultures are in bold.

smooth– and thin–walled, (3–)4–5(–6) µm long, $\bar{x}$ ± SD = 4 ± 0.7 µm; three median cells doliiform, concolourous, pale brown, somewhat verruculose, (10–)11–14(–16) µm long, $\bar{x}$ ± SD = 13 ± 1.3 µm (the second cell from base (3–)4–5(–6) µm long, $\bar{x}$ ± SD = 4 ± 0.6 µm; third cell 3–4(–5) µm long, $\bar{x}$ ± SD = 4 ± 0.5 µm; fourth cell (3–)4–5 µm long, $\bar{x}$ ± SD = 4 ± 0.4 µm), wall of the third and fourth cell from the base thicker than that of the second cell, septa darker than the rest of the cells; apical cell cylindrical to subcylindrical, conic, hyaline, smooth- and thin-walled, (2–)3–4 µm long, $\bar{x}$ ± SD = 3 ± 0.6 µm; with 2–3 tubular apical appendages (mostly 2), arising from the apical crest, filiform, unbranched, (8–)11–16(–20) µm long, $\bar{x}$ ± SD = 14 ± 3.0 µm; basal appendage single, unbranched, centric or excentric, (2–)3–5(–6) µm long, $\bar{x}$ ± SD = 4 ± 1.0 µm.

Colony characteristics – Colony on PDA reaching 60 mm diam after 6d at 25 °C, circular, effuse with floccose texture, margin crenate and filamentous, colour white, with aerial mycelia on the surface, with immersed to semi-immersed conidiomata, producing black, glistening spore mass; reverse pale honey-coloured, slightly concentric, with black conidiomata.

Materials examined – TAIWAN, Taipei Botanical Garden, Zhongzheng district, Taipei city, on dead grass (Poaceae) 9 August 2017, I Tsai, BG11.1 (NTUH 17–009; holotype) –ex–holotype living culture (NTUCC 17–009). *ibid*. (NTUH 17–010; paratype) –ex–paratype living culture (NTUCC 17–010).

Notes – *Pestalotiopsis formosana* is a unique taxon based on both morphology and phylogeny (Figs 1, 2). *Pestalotiopsis formosana* differs from its phylogenetically closely related species *P. parva* by the number of apical appendages (mostly two versus mostly three), relatively longer apical appendages (11–16 µm versus 6.5–12 µm), and host (Poaceae versus Ericaceae or Fabaceae).

Pestalotiopsis neolitseae Ariyawansa & K.D. Hyde, sp. nov.,

MycoBank number: MB827598; Facesoffungi number: FoF04938

Etymology – The specific epithet *neolitseae* is based on the host genus *Neolitsea*.

Pathogenic causing spots on leaves of *Neolitsea villosa*. Leaf spots circular to irregular, grey with brown margins when mature, or covering up to half of the leaf; dotted with acervuli. Sexual morph: undetermined. Asexual morph: *Conidiomata* on PDA pycnidial, globose or lenticular, solitary or aggregate, immersed or semi-immersed, exuding black slimy conidial mass on the surface of mycelia. *Conidiophores* often reduce to conidiogenous cells, when present, branched or unbranched. *Conidiogenous cell* discrete or integrated, cylindrical to subcylindrical, hyaline, smooth, often tapering to a neck on the septum of developing conidia, (6–)7–11(–13) × (2–)2–4(–5) µm, $\bar{x}$ ± SD = 9 ± 2.2 × 3 ± 0.9 µm. *Conidia* ellipsoid, fusoid, straight to slightly curved, 4-septate, (15–)18–21(–25) × (4–)5–6 µm, $\bar{x}$ ± SD = 20 ± 1.9 × 6 ± 0.4 µm; basal cell obconic, hyaline, smooth- and thin-walled, (3–)3–5(–6) µm long, $\bar{x}$ ± SD = 4 ± 0.7 µm; three median cells doliiform, concolourous, pale brown, somewhat verruculose, (10–)11–14(–14) µm long, $\bar{x}$ ± SD = 12 ± 1.2 µm (the second cell from base 3–4(–5) µm long, $\bar{x}$ ± SD = 4 ± 0.4 µm; third cell 3–4(–5) µm long, $\bar{x}$ ± SD = 4 ± 0.4 µm; fourth cell 4–5(–6) µm long, $\bar{x}$ ± SD = 4 ± 0.4 µm), wall of the third and fourth cell from the base thicker than that of the second cell, septa darker than the rest of the cells; apical cell cylindrical to subcylindrical, conic to bell-shaped, hyaline, smooth- and thin-walled, (2–)3–4(–6) µm long, $\bar{x}$ ± SD = 3 ± 0.5 µm; with 1–3 tubular apical appendages (mostly 2), arising from the apical crest, filiform, unbranched or branched, (7–)10–15(–17) µm long, $\bar{x}$ ± SD = 13 ± 2.5 µm; basal appendage single, unbranched, straight to curved, centric or excentric, 2–5(–6) µm long, $\bar{x}$ ± SD = 4 ± 0.9 µm.

Colony characteristics – Colony on PDA reaching 75mm diam after 6d at 25°C, circular, effuse with floccose texture, margin crenated and filamentous, colour white, with aerial mycelia on the surface, with immersed to semi-immersed conidiomata, producing black, glistening spore mass; reverse colour whitish pink, centre pale brown, margin pale honey–coloured, with black conidiomata.

Material examined – TAIWAN, Taipei Botanical Garden, Zhongzheng district, Taipei city, on leaf of *Neolitsea villosa* (Lauraceae) 9 August 2017, H. A. Ariyawansa, BG2.2 (NTUH 17-011; holotype) – ex–holotype living culture (NTUCC 17-011). *ibid*. (NTUH 17-012; paratype) – ex–paratype living culture (NTUCC 17–012).

Notes – *Pestalotiopsis neolitseae* is typical of *Pestalotiopsis* in having concolourous median cells and proposed here as a distinctive taxon based phylogeny together with morphology (Figs 1, 3). *Pestalotiopsis neolitseae* differs from *P. jinchanghensis* in having smaller conidia (18–21 ×5–6 µm versus 22–32 × 5.5–8.5 µm), shorter apical appendages (10–15 µm versus 15–33.5 µm) and shorter basal appendages (2–5 µm versus 5.5–15.5 µm). Furthermore, *Pestalotiopsis neolitseae* differs from *P. jinchanghensis* by host (*Neolitsea* versus *Camellia*), and the geographical location (Taiwan versus mainland China).

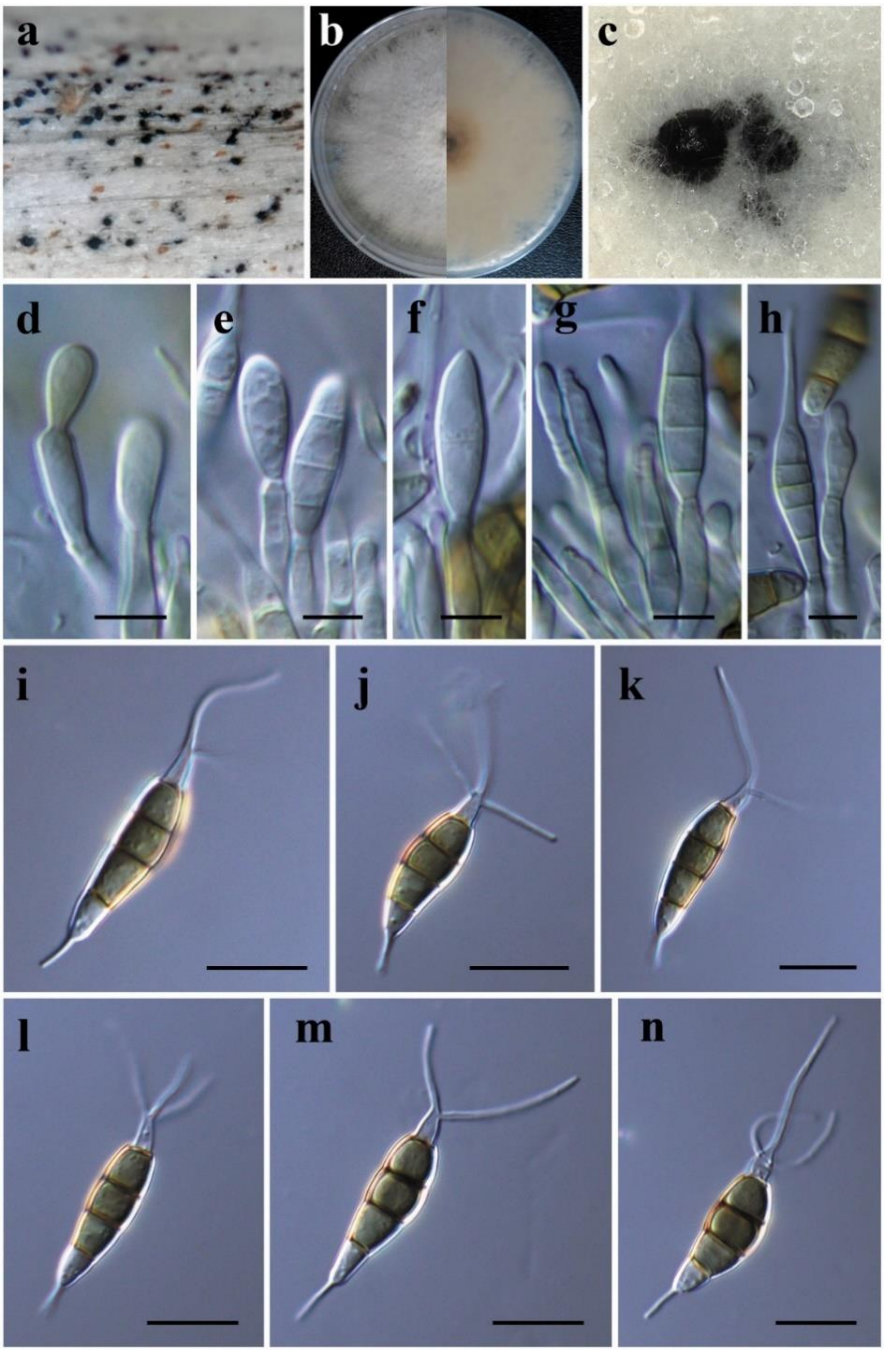

Figure 2 – *Pestalotiopsis formosana* (holotype). a Immersed conidiomata on host. b Surface and lower sight of colonies on PDA. c Conidioma on PDA. d–h Conidiogenous cells. i–n Conidia. Scale bars: d–h 5 µm, i–n 10 µm.

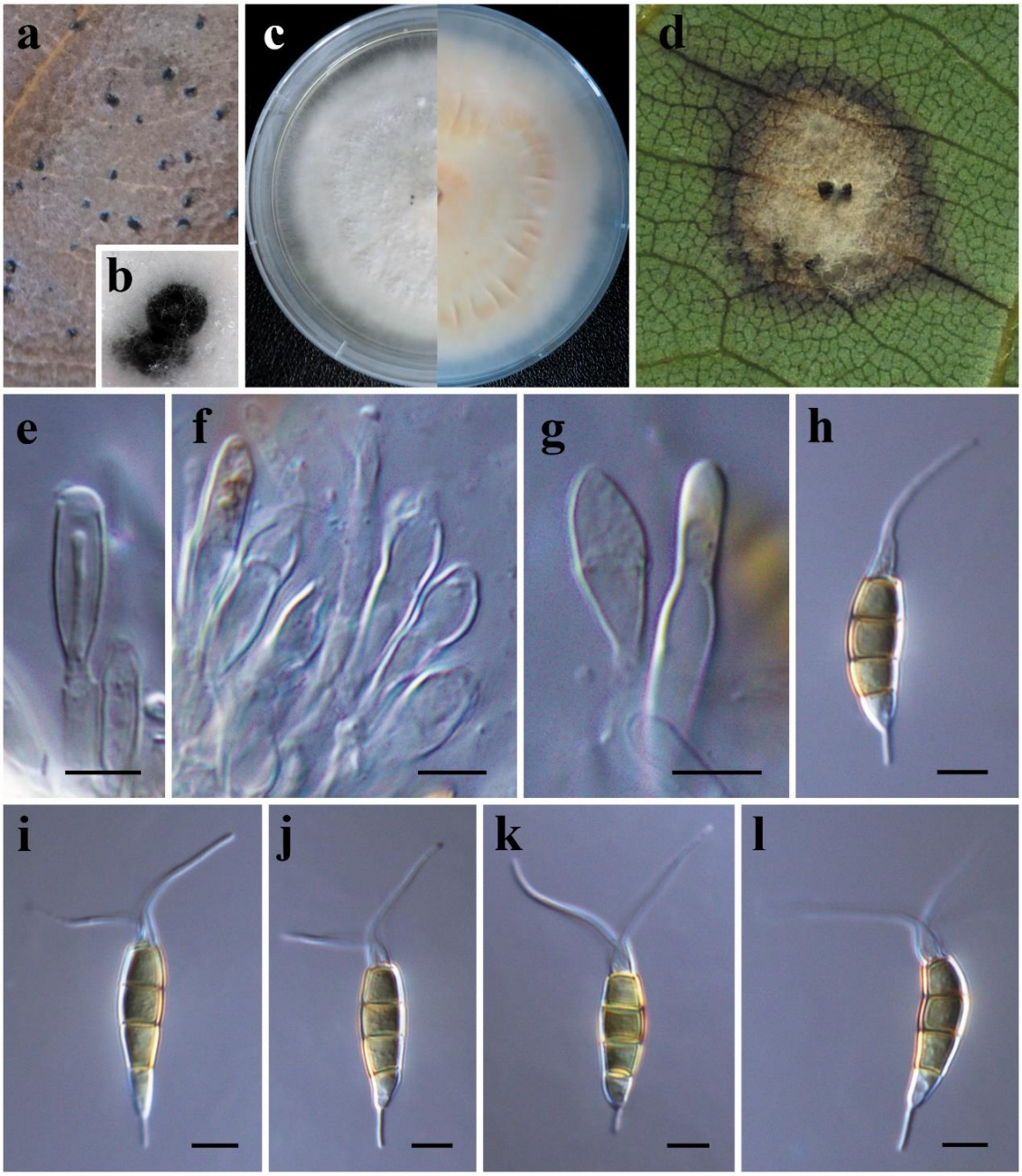

Figure 3 – *Pestalotiopsis neolitseae* (holotype). a, d *Neolitsea villosa* leaves with characteristic leaf spots. b Conidioma on PDA. c Surface and lower view of colonies on PDA. e–h Conidiogenous cells. i–l Conidia. Scale bars: d–k 5µm.

Pathogenicity test

Results of pathogenicity test revealed that, with wound inoculation, *Pestalotiopsis neolitseae* was pathogenic on *Neolitsea villosa* leaves (Fig. 3a, d) and the symptoms induced were similar to those, which occur under natural conditions in the field. The wounded *Neolitsea villosa* leaves initially developed small, circular, ash–coloured spots, which later changed into brown spots. After 18 days of incubation, the spots prolonged to 5 mm diam. The spots further enlarged and became sunken causing soft decay of the leaf tissues, covered by white mycelia (Fig. 3d). In contrast, symptoms were not observed on non–wounded leaves, signifying that wounding may be essential for symptom development. The experiment was done using three replicates and repeated three times. The fungus was re–isolated from lesions of the diseased leaves with 100% frequency, and its morphological features and gene sequences were equal to the original ones, which definite that *Pestalotiopsis neolitseae* is the causal agents for *Neolitsea villosa* leaf spot disease.

Discussion

Data acquired by traditional morphological recognition of conidial characters are inadequate when identifying species as well as the genus limits in pestalotioid taxa (Ariyawansa et al. 2018, Tsai et al. 2018, Liu et al. 2017, Nozawa et al. 2017, Maharachchikumbura et al. 2013, 2014). Although the morphological recognition of *Pestalotiopsis sensu stricto*, *Pseudopestalotiopsis* and *Neopestalotiopsis* rely on the conidiogenous cells and colour of their median conidial cells, some of the *Pestalotiopsis*–like species have shown overlapping morphologies of conidiogenous cells and median cell colour (Liu et al. 2017, Nozawa et al. 2017). Therefore, molecular-based polyphasic approaches are essential to recognise the species as well as the generic boundaries of pestalotioid taxa (Ariyawansa et al. 2018, Tsai et al. 2018, Liu et al. 2017, Maharachchikumbura et al. 2014, 2016a, b, Nozawa et al. 2017).

The present survey illustrates two novel species of *Pestalotiopsis sensu stricto* considering both morphology and phylogeny. The phylogenetic construction of the DNA sequences of single and combined ITS, *tub2* and *tef1* genes provide robust confirmation that *Pestalotiopsis formosana* and *P. neolitseae* fit in *Pestalotiopsis sensu stricto* and they form separate linages showing the new taxa are separated from other species of the genus with high bootstrap support (Fig. 1). Moreover, we outlined the characters of *Pestalotiopsis* taxa, which are phylogenetically related to *Pestalotiopsis formosana* and *P. neolitseae* in Supplementary Table 2. In addition, our study expands knowledge on the diversity of pestalotioid species in Taiwan and to best of our understanding, this is the first record of *Pestalotiopsis* species from *Neolitsea villosa* in Taiwan.

Acknowledgements

This study was partially funded by the Ministry of Science and Technology, Taiwan (MOST project ID: 106–2621–B–002–005–MY2). We appreciate the support given by Dr. Wei–Fan SU, the director of the Taipei Botanical Gardens, Professors Ting-Hsuan Hung, Ruey–Fen Liou, Chan-Pin Lin, Wei–Chiang Shen, Associate Professor Ying–Lien Chen and Ms. Ichen Tsai. We are grateful to A.D. Ariyawansa, D.M.K. Ariyawansa, Ruwini Ariyawansa, Amila Gunasekara and Oshen Chemika for their valuable suggestions.

References

Ariyawansa HA, Hawksworth DL, Hyde KD, Jones EBG et al. 2014 – Epitypification and neotypification: guidelines with appropriate and inappropriate examples. Fungal Diversity 69, 57–91

Ariyawansa HA, Hyde KD, Liu JK, Wu SP, Liu ZY. 2016a – Additions to Karst Fungi 1: *Botryosphaeria minutispermatia* sp. nov., from Guizhou Province, China. Phytotaxa 275, 35–44

Ariyawansa HA, Hyde KD, Thambugala KM, Maharachchikumbura SSN et al. 2016b – Additions to Karst Fungi 2: *Alpestrisphaeria jonesii* from Guizhou Province, China. Phytotaxa 277, 255–265.

Ariyawansa HA, Tsai I, Jones EGB. 2018 – A new cryptic species of *Pseudopestalotiopsis* from Taiwan. Phytotaxa 357(2), 133–140.

Chen Y, Zeng L, Shu N, Jiang M et al. 2018 – *Pestalotiopsis*-like species causing gray blight disease on *Camellia sinensis* in China. Plant Disease 102(1), 98–106

Dettman JR, Jacobson DJ, Turner E, Pringle A, Taylor JW. 2003 – Reproductive isolation and phylogenetic divergence in *Neurospora*: comparing methods of species recognition in a model eukaryote. Evolution 57, 2721–2741.

Glass NL, Donaldson GC. 1995 – Development of primer sets designed for use with the PCR to amplify conserved genes from filamentous ascomycetes. Applied and Environmental Microbiology 61, 1323–1330.

Huelsenbeck JP, Ronquist F, Hall B. 2003 – MrBayes: a program for the Bayesian inference of phylogeny. Version 3.0 b4.

Jayasiri SC, Hyde KD, Ariyawansa HA, Bhat DJ et al. 2015 – The faces of fungi database: fungal names linked with morphology, phylogeny and human impacts. Fungal Diversity 74, 3–18.
Jeewon R, Hyde KD. 2016 – Establishing species boundaries and new taxa among fungi: recommendations to resolve taxonomic ambiguities. Mycosphere 7(11), 1669–1677.
Liu F, Hou L, Raza M, Cai L. 2017 – *Pestalotiopsis* and allied genera from *Camellia*, with description of 11 new species from China. Scientific Reports 7(1), 866.
Maharachchikumbura SSN, Guo LD, Chukeatirote E, Hyde KD. 2013 – Improving the backbone tree for the genus *Pestalotiopsis*; addition of *P. steyaertii* and *P. magna* sp. nov. Mycological Progress 13, 617–624.
Maharachchikumbura SSN, Guo LD, Liu ZY, Hyde KD. 2016b – *Pseudopestalotiopsis ignota* and *Ps. camelliae* spp. nov. associated with grey blight disease of tea in China. Mycological Progress 15, 22.
Maharachchikumbura SSN, Hyde KD, Groenewald JZ, Xu J, Crous P. 2014 – *Pestalotiopsis* revisited. Studies in Mycology 79, 121–186
Maharachchikumbura SSN, Hyde KD, Jones EBG, McKenzie EHC et al. 2016a – Families of Sordariomycetes. Fungal Diversity 79, 1–317.
Miller MA, Pfeiffer W, Schwartz T. 2010 – Creating the CIPRES Science Gateway for inference of large phylogenetic trees. In Gateway Computing Environments Workshop (GCE), 2010 (pp. 1–8). Ieee.
Nozawa S, Yamaguchi K, Van Hop D, Phay N et al. 2017 – Identification of two new species and a sexual morph from the genus *Pseudopestalotiopsis*. Mycoscience 58(5), 328–337.
Nylander J. 2004 – MrModeltest v2. Program distributed by the author, Evolutionary Biology Centre, Uppsala University, Uppsala, Sweden.
O'Donnell K, Cigelnik E. 1997 – Two divergent intragenomic rDNA ITS2 types within a monophyletic lineage of the fungus Fusarium are nonorthologous. Molecular Phylogenetics and Evolution 7, 103–116.
Page RD. 2001 – TreeView Glasgow University, Glasgow, UK
Rambaut A, Drummond AJ. 2007 – Tracer v1, 4. Available from: http://beast. bio. ed. ac. uk/Tracer (accessed 10 December 2017).
Rambaut A, Drummond AJ. 2008 – FigTree: Tree figure drawing tool, version 1.2. 2.
Rannala B, Yang Z. 1996 – Probability distribution of molecular evolutionary trees: a new method of phylogenetic inference. Journal of Molecular Evolution 43, 304–311.
Rehner S. 2001 – Primers for elongation factor 1–α (EF1–α).
Schoch CL, Seifert KA, Huhndorf S, Robert V et al. 2012 – Nuclear ribosomal internal transcribed spacer (ITS) region as a universal DNA barcode marker for Fungi. Proceedings of the National Academy of Sciences 109, 6241–6246.
Stamatakis A. 2014 – RAxML version 8: a tool for phylogenetic analysis and post-analysis of large phylogenies. Bioinformatics 30, 1312–1313.
Steyaert RL. 1949 – Contributions al'etude monographique de *Pestalotia* de Not. et Monochaetia Sacc. (*Truncatella* gen. nov. et *Pestalotiopsis* gen. nov.). Bulletin Jardin Botanique Etat Bruxelles 19, 285–354.
Stielow B, Bubner B, Hensel G, Munzenberger B et al. 2010 – The neglected hypogeous fungus *Hydnotrya bailii* Soehner (1959) is a widespread sister taxon of *Hydnotrya tulasnei* (Berk.) Berk. and Broome (1846). Mycological Progress 9, 195–203.
Tamura K, Peterson D, Peterson N, Stecher G et al. 2011 – MEGA5: molecular evolutionary genetics analysis using maximum likelihood, evolutionary distance, and maximum parsimony methods. Molecular Biology and Evolution 28, 2731–2739.
Taylor JW, Jacobson DJ, Kroken S, Kasuga T et al. 2000 – Phylogenetic species recognition and species concepts in fungi. Fungal Genetics and Biology 31, 21–32.
Tsai I, Maharachchikumbura SSN, Hyde KD, Ariyawansa HA. 2018 – Molecular phylogeny, morphology and pathogenicity of *Pseudopestalotiopsis* species of *Ixora* in Taiwan. Mycological Progress 17, 941–952.

White TJ, Bruns TD, Lee S, Taylor J. 1990 – Amplification and direct sequencing of fungal ribosomal RNA genes for phylogenetics. PCR protocols: a guide to methods and applications 18, 315–322.
Wijayawardene NN, Hyde KD, Rajeshkumar KC, Hawksworth DL et al. 2017 – Notes for genera: Ascomycota. Fungal Diversity 86, 1–594.
Wijayawardene NN, Hyde KD, Lumbsch HT, Liu JK et al. 2018 – Outline of Ascomycota – 2017. Fungal Diversity 88, 167-263.
Zhaxybayeva O, Gogarten JP. 2002 – Bootstrap, Bayesian probability and maximum likelihood mapping: exploring new tools for comparative genome analyses. BMC genomics 3, 4.

Supplementary Table 1 Details of the isolates used in the phylogenetic tree. Newly generated sequences are in red.

Taxon	**Strain ID**	**ITS**	***tub***	***tef***
Pestalotiopsis kenyana	CBS 442.67	KM199302	KM199395	KM199502
Pestalotiopsis trachicarpicola	OP143	JQ845947	JQ845945	JQ845946
Pestalotiopsis oryzae	CBS 353.69	KM199299	KM199398	KM199496
Pestalotiopsis oryzae	CBS 111522	KM199294	KM199394	KM199493
Pestalotiopsis rhodomyrtus	LC3413	KX894981	KX895313	KX895198
Pestalotiopsis rhodomyrtus	HGUP4230	KF412648	KF412642	KF412645
Pestalotiopsis rhodomyrtus	LC4458	KX895010	KX895342	KX895228
Pestalotiopsis telopeae	CBS 113606	KM199295	KM199402	KM199498
Pestalotiopsis telopeae	CBS 114161	KM199296	KM199403	KM199500
Pestalotiopsis telopeae	CBS 114137	KM199301	KM199469	KM199559
Pestalotiopsis macadamiae	BRIP 63739a	KX186589	KX186681	KX186622
Pestalotiopsis macadamiae	BRIP 63738b	KX186588	KX186680	KX186621
Pestalotiopsis australasiae	CBS 114126	KM199297	KM199409	KM199499
Pestalotiopsis australasiae	CBS 114141	KM199298	KM199410	KM199501
Pestalotiopsis sp.	LC3637	KX894993	KX895324	KX895210
Pestalotiopsis sp.	LC3640	KX894995	KX895326	KX895212
Pestalotiopsis brachiata	LC2988	KX894933	KX895265	KX895150
Pestalotiopsis brachiata	LC8188	KY464142	KY464162	KY464152
Pestalotiopsis biciliata	CBS 236.38	KM199309	KM199401	KM199506
Pestalotiopsis biciliata	CBS 124463	KM199308	KM199399	KM199505
Pestalotiopsis sp.	LC3616	KX894990	KX895321	KX895207
Pestalotiopsis knightiae	CBS 111963	KM199311	KM199406	KM199495
Pestalotiopsis knightiae	CBS 114138	KM199310	KM199408	KM199497
Pestalotiopsis grevilleae	CBS 114127	KM199300	KM199407	KM199504
Pestalotiopsis formosana	NTUCC 17-009	MH809381	MH809385	MH809389
Pestalotiopsis formosana	NTUCC 17-010	MH809382	MH809386	MH809390
Pestalotiopsis parva	CBS 278.35	KM199313	KM199405	KM199509
Pestalotiopsis parva	CBS 265.37	KM199312	KM199404	KM199508
Pestalotiopsis rosea	MFLUCC 12-0258	JX399005	JX399036	JX399069
Pestalotiopsissp digitalis	MFLU 14–0208	KP781879	KP781883	

Supplementary Table 1 Continued.

Taxon	Strain ID	ITS	*tub*	*tef*
Pestalotiopsissp dracontomelon	MFLU 14–0207			KP781880
Pestalotiopsis adusta	ICMP 6088	JX399006	JX399037	JX399070
Pestalotiopsis adusta	MFLUCC 10-0146	JX399007	JX399038	JX399071
Pestalotiopsis papuana	CBS 887.96	KM199318	KM199415	KM199492
Pestalotiopsis papuana	CBS 331.96	KM199321	KM199413	KM199491
Pestalotiopsis sp.	CBS 263.33	KM199316	KM199414	KM199489
Pestalotiopsis sp.	CBS 264.33	KM199322	KM199412	KM199490
Pestalotiopsis malayana	CBS 102220	KM199306	KM199411	KM199482
Pestalotiopsis diploclisia	CBS 115585	KM199315	KM199417	KM199483
Pestalotiopsis diploclisia	CBS 115587	KM199320	KM199419	KM199486
Pestalotiopsis diploclisia	CBS 115449	KM199314	KM199416	KM199485
Pestalotiopsis humus	CBS 336.97	KM199317	KM199420	KM199484
Pestalotiopsis humus	CBS 115450	KM199319	KM199418	KM199487
Pestalotiopsis licualacola	HGUP4057	KC492509	KC481683	KC481684
Pestalotiopsis aggestorum	LC8186	KY464140	KY464160	KY464150
Pestalotiopsis aggestorum	LC6301	KX895015	KX895348	KX895234
Pestalotiopsis colombiensis	CBS 118553	KM199307	KM199421	KM199488
Pestalotiopsis jinchanghensis	LC6636	KX895028	KX895361	KX895247
Pestalotiopsis jinchanghensis	LC8190	KY464144	KY464164	KY464154
Pestalotiopsis neolitseae	NTUCC 17-011	MH809383	MH809387	MH809391
Pestalotiopsis neolitseae	NTUCC 17-012	MH809384	MH809388	MH809392
Pestalotiopsis dilucida	LC3232	KX894961	KX895293	KX895178
Pestalotiopsis dilucida	LC8184	KY464138	KY464158	KY464148
Pestalotiopsis australis	CBS 114193	KM199332	KM199383	KM199475
Pestalotiopsis australis	CBS 111503	KM199331	KM199382	KM199557
Pestalotiopsis yunnanensis	HMAS 96359	AY373375		
Pestalotiopsis scoparia	CBS 176.25	KM199330	KM199393	KM199478
Pestalotiopsis jiangxiensis	LC4399	KX895009	KX895341	KX895227
Pestalotiopsis jinchanghensis	LC4242	KX895035	KX895327	KX895213
Pestalotiopsis unicolor	MFLUCC 12-0275	JX398998	JX399029	JX399063
Pestalotiopsis unicolor	MFLUCC 12-0276	JX398999	JX399030	-
Pestalotiopsis intermedia	MFLUCC 12-0259	JX398993	JX399028	JX399059
Pestalotiopsis linearis	MFLUCC 12-0271	JX398992	JX399027	JX399058
Pestalotiopsis chamaeropis	CBS 186.71	KM199326	KM199391	KM199473
Pestalotiopsis chamaeropis	CBS 113607	KM199325	KM199390	KM199472
Pestalotiopsis hollandica	CBS 265.33	KM199328	KM199388	KM199481
Pestalotiopsis brassicae	CBS 170.26	KM199379		KM199558

Supplementary Table 1 Continued.

Taxon	Strain ID	ITS	*tub*	*tef*
Pestalotiopsis verruculosa	MFLUCC 12-0274	JX398996		JX399061
Pestalotiopsis sequoiae	MFLUCC 13-0399	KX572339		
Pestalotiopsis monochaeta	CBS 144.97	KM199327	KM199386	KM199479
Pestalotiopsis monochaeta	CBS 440.83	KM199329	KM199387	KM199480
Pestalotiopsis italiana	MFLUCC 12-0657	KP781878	KP781882	KP781881
Pestalotiopsis lushanensis	LC4344	KX895005	KX895337	KX895223
Pestalotiopsis lushanensis	LC8182	KY464136	KY464156	KY464146
Pestalotiopsis rhododendri	IFRDCC 2399	KC537804	KC537818	KC537811
Pestalotiopsis clavata	MFLUCC 12-0268	JX398990	JX399025	JX399056
Pestalotiopsis inflexa	MFLUCC 12-0270	JX399008	JX399039	JX399072
Pestalotiopsis portugalica	CBS 393.48	KM199335	KM199422	KM199510
Pestalotiopsis portugalica	LC2929	KX894921	KX895253	KX895138
Pestalotiopsis yanglingensis	LC4553	KX895012	KX895345	KX895231
Pestalotiopsis yanglingensis	LC3067	KX894949	KX895281	KX895166
Pestalotiopsis camelliae	MFLUCC 12-0277	JX399010	JX399041	JX399074
Pestalotiopsis camelliae	CBS 443.62	KM199336	KM199424	KM199512
Pestalotiopsis furcata	MFLUCC 12-0054	JQ683724	JQ683708	JQ683740
Pestalotiopsis furcata	LC6303	KX895016	KX895349	KX895235
Pestalotiopsis sp.	LC6576	KX895021	KX895354	KX895240
Pestalotiopsis longiappendiculata	LC3013	KX894939	KX895271	KX895156
Pestalotiopsis novaehollandiae	CBS 130973	KM199337	KM199425	KM199511
Pestalotiopsis gaultheria	OP137	KC537805	KC537819	KC537812
Pestalotiopsis spathulata	CBS 356.86	KM199338	KM199423	KM199513
Pestalotiopsis diversiseta	MFLUCC 12-0287	JX399009	JX399040	JX399073
Pestalotiopsis arengae	CBS 331.92	KM199340	KM199426	KM199515
Pestalotiopsis hawaiiensis	CBS 114491	KM199339	KM199428	KM199514
Pestalotiopsis arceuthobii	CBS 434.65	KM199341	KM199427	KM199516
Pestalotiopsis anacardiacearum	IFRDCC 2397	KC247154	KC247155	KC247156
Pestalotiopsis jesteri	CBS 109350	KM199380	KM199468	KM199554
Neopestalotiopsis saprophyta	MFLUCC-12-0282	JX398982	JX399017	JX399048

Supplementary Table 2 A summary of characters of species of *Pestalotiopsis*

Pestalotiopsis Species	**Conidiogenous cells (µm)**	**Conidia size (µm)**	**No. of apical appendages**	**Branched or unbranched**	**Length of apicalappendages (µm)**	**No. of basal appendages**	**Branched or unbranched**	**Length of basal appendages (µm)**	**Reference**
P. formosana	(5–)9–15(–19) × (2–)2–3(–4)	(15–)18–22(–26) × (5–)6–7(–7)	2–3 (mostly 2)	unbranched	(8–)11–16(–20)	**1**	unbranched	**(2–)3–5(–6)**	This study
P. neolitseae	(6–)7–11(–13) × (2–)2–4(–5)	(15–)18–21(–25) × (4–)5–6(–6)	1–3 (mostly 2)	unbranched	(7–)10–15(–17)	1	unbranched	2–5	This study
P. jinchanghensis	5–12 × 2–7	22–32 × 5.5–8.5	1–3 (mostly 2)	unbranched	15–33.5	1–2	unbranched	5.5–15.5	Liu et al. 2017
P. parva	5–18 × 2–4	(16–)16.5–20(–21) × 5–7(–7.5)	2–3 (mostly 3)	unbranched	(6–)6.5–12(–13)	1	unbranched	2–4	Liu et al. 2017
P. maculans	5–15 × 2–4	19–27.5 × 6–8.5	2–3	unbranched	3–4	1	unbranched	1.5–3	Nag Raj 1985